Nanoscale Res Lett (2010) 5:1442–1448
DOI 10.1007/s11671-010-9659-1

NANO EXPRESS

Stable White Light Electroluminescence from Highly Flexible Polymer/ZnO Nanorods Hybrid Heterojunction Grown at 50°C

A. Zainelabdin · S. Zaman · G. Amin · O. Nur · M. Willander

Received: 7 April 2010 / Accepted: 24 May 2010 / Published online: 4 June 2010

Abstract Stable intrinsic white light–emitting diodes were fabricated from c-axially oriented ZnO nanorods (NRs) grown at 50°C via the chemical bath deposition on top of a multi-layered poly(9,9-dioctylfluorene-co–*N*-(4-butylpheneylamine)diphenylamine)/poly(9,9dioctyl-fluorene) deposited on PEDOT:PSS on highly flexible plastic substrate. The low growth temperature enables the use of a variety of flexible plastic substrates. The fabricated flexible white light–emitting diode (FWLED) demonstrated good electrical properties and a single broad white emission peak extending from 420 nm and up to 800 nm combining the blue light emission of the polyflourene (PFO) polymer layer with the deep level emission (DLEs) of ZnO NRs. The influence of the temperature variations on the FWLED white emissions characteristics was studied and the devices exhibited high operation stability. Our results are promising for the development of white lighting sources using existing lighting glass bulbs, tubes, and armature technologies.

Keywords Hybrid technology · ZnO nanorods · Polymers · Large area lighting · Flexible low temperature LEDs

A. Zainelabdin (✉) · S. Zaman (✉) · G. Amin · O. Nur · M. Willander
Department of Science and Technology, Linköping University, 601 74 Norrköping, Sweden
e-mail: ahmza@itn.liu.se

S. Zaman
e-mail: saiza@itn.liu.se

Introduction

Zinc oxide (ZnO) is a II–VI semiconductor material with a wide bandgap of about (3.37 eV) together with a high exciton binding energy of (60 meV) both at room temperature rendering ZnO to receive global attention especially in connection with the emerging nanotechnology paces toward functionality [1]. Moreover, ZnO possesses deep levels that emit light covering the whole visible spectrum [2]. ZnO nanostructures family has gained substantial interest due to their simple fabrication routes, along with low cost and self organization growth behavior enabling the growth of ZnO nanostructures on any substrate material regardless of lattice matching issues [3]. Many groups have fabricated and studied ZnO nanorod-based devices including LEDs e.g. by our group recently [2–7], random laser based on ZnO nanorods has also been demonstrated and showed a potential of ZnO for photonics applications [8]. The most challenging problem of ZnO-based photonic devices is the lack of stable and reliable p-type doping; mainly due to the self compensation property of ZnO [8]. Therefore, using heterojunction strategy for photonic devices based on ZnO nanorods (NRs) has been a feasible way to obtain good performance LED based on ZnO NRs [2–7].

Organic polymers light-emitting diodes (PLED) have been intensively investigated for optoelectronic applications such as flat panel displays and solar cell, to name a few. The main advantageous features of polymer-based devices are low cost, low power consumption, and simple processability etc. Due to the self organized growth property of ZnO, it is possible to grow ZnO nanorods on polymeric substrates. The combination of ZnO NRs and polymers to form hybrid junction will add the advantage of achieving large area LEDs using a single contact, which is

an advantage not possible to gain by using PLED configuration. The first hybrid organic/ZnO NRs LED has been reported by Könenkamp et al. [9], their LED composed of electrodeposited ZnO NRs on F-doped SnO_2 glass substrate acting as a cathode and applying PEDOT:PSS as a p-type contact [9]. Although the device demonstrated rational LED characteristics, it has a drawback regarding stability [9]. White light–emitting diodes based on organic/ZnO NRs have also been studied by our group [4, 6, 7] different multilayer and blended polymers were utilized to fabricate LEDs on glass substrates. In those studies, ZnO NRs were grown at a temperature of 95°C, and the emitted light was dominated by the polymer emissions (mainly the blue line) leading to bluish white emission LEDs [4, 6, 7]. Fabrication of white organic/inorganic LEDs on flexible substrates on the other hand represents an additional step toward the realization of ZnO/polymer hybrid heterojunctions LEDs. Nevertheless, there are many issues to be solved to achieve this goal. For instance, the growth temperature of ZnO NRs has to be lowered to a large extent to permit the fabrication of LEDs on flexible substrates. It is important to mention that all published results on hybrid organic/ZnO NRs heterojunctions white electroluminescence (EL) were obtained for cases where the growth was performed at 80°C or higher [4, 6, 7, 9–11]. Moreover, it is of interest to demonstrate a white EL from such hybrid heterojunctions at lower temperatures, to enable the use of a variety of flexible plastic as a substrate. Such achievement will lead to the possibility of integrating this class of white LEDs with existing glass bulbs, tubes, and armature technologies.

In this paper, a novel stable white light–emitting diode fabricated on highly flexible plastic substrate is reported. This flexible white light–emitting diode (FWLED) was fabricated on commercial PEDOT:PSS flexible plastic and composed of a vertically aligned ZnO NRs grown by chemical bath deposition route at a low temperature of 50°C, on multi-layered blue emitting polymer poly(9,9-dioctyl-fluorene) (PFO) and hole transporting polymer poly(9,9-dioctylfluorene-co–*N*-(4-butylpheneyl-amine)diphenylamine) (TFB) in between the PFO and the PEDOT:PSS. The highly flexible and stretchable light-emitting diode yielded a stable white broad emission band covering the entire visible spectrum.

Experimental Approach

All materials used in the growth of ZnO nanorods were purchased from (Sigma–Aldrich) and were applied as-received without further purification. The PFO and TFB polymers were purchased from American Dye Source, Canada. All polymer solutions were prepared by dissolving 4 mg/ml in toluene. A commercial PEDOT:PSS on plastic foil was chosen as a substrate in the subsequent fabrication of the hybrid LED due to the facts that the PEDOT:PSS on plastic is flexible, transparent to the visible light with reasonable electrical properties and can be used for large-scale production.

The LED fabrication started by thoroughly cleaning the PEDOT:PSS substrate with acetone and iso-propanol under sonication for 3 min. Then, the TFB hole transporting solution was spun coated at 1,500 rpm for 30 s, followed by baking for 10 min at 75°C to evaporate the residual toluene. The PFO which is a blue luminescent polymer was then spun coated on top of the TFB layer at spin speed of 2,000 rpm for 30 s and cured for 15 min at 75°C. After that, the growth of the ZnO nanorods was carried out by spin coating ZnO nanoparticles (NPs) solution prepared following the method developed by Pacholski et al. [12]. This coating process was applied three times and a rational coverage is expected. The deposition of ZnO nanorods was conducted through a chemical bath deposition method at 50°C temperature. In brief, Zinc Nitrate Hexahydrate ($Zn(NO_3)_2 \cdot 6H_2O$) was dissolved in 100 mL DI-water to achieve 0.15 M concentration, and (0.1 M) of Hexamethylenetetramine (HMT, $C_6H_{12}N_4$) in 100 mL DI-water. The pre-coated substrates were transferred to the aqueous solution and the whole Pyrex beaker was kept for several hours at 50°C in traditional laboratory oven. Details of the growth will be published somewhere else [13]. After growth, the samples were thoroughly soaked in DI-water under ultrasonic agitation to remove the un-reacted salts, and then left to dry at room temperature. Prior to the contact deposition, a photoresist (S1818) was spun coated to insulate the ZnO NRs from each other at spin speed of 3,000 rpm for 30 s and then cured at 90°C for 2 min. Standard oxygen reactive ion etching (RIE) was then employed to partly etch the upper part of the photoresist that covers ZnO NRs tips. The last step in the fabrication of the hybrid LED was to utilize a metal contact to both parts of the hybrid junction. For the ZnO, ohmic contact was achieved by thermally evaporating (Au/Ti 20 nm/10 nm) on top of the fabricated device. Schematic illustrations of the hybrid LED is shown in Fig. 1a. A simple silver paste was used to act as a bottom contact to the PEDOT:PSS substrate.

All measurements on the fabricated hybrid LED device were performed at room ambient conditions, only in the case of temperature stability the measurements were carried out at different temperatures. Field emission scanning electron microscopy (SEM) was used to study the morphology of the grown ZnO NRs. Room temperature photoluminescence (PL) was investigated using (coherent MBD 266) with $\lambda = 266$ nm as excitation source, and the PL spectra were collected with a CCD detector. The

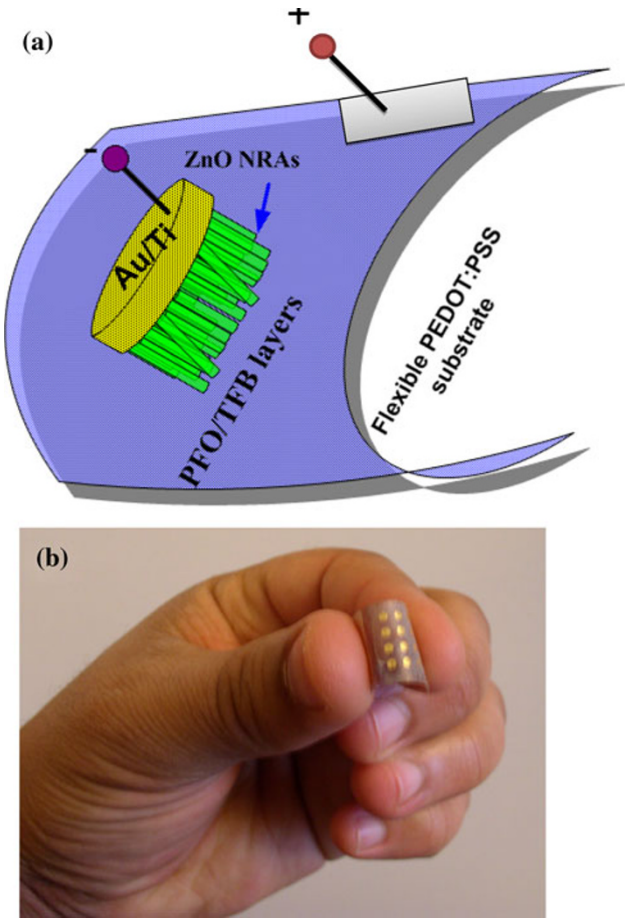

Fig. 1 **a** A schematic diagram of the flexible white light–emitting diode (*FWLED*) showing the different parts of the device, and in **b** a digital photograph of the flexible PEDOT:PSS substrate containing 20 FWLEDs bent at large angle of around 60°

current–voltage (*I–V*) characteristics were measured with Agilent 4155B semiconductor parameter analyzer. The EL behavior of the fabricated FWLED device was examined with Keithley 2400 source meter, while the EL spectra were assembled via Andor Shamrock 303iB spectrometer supported with Andor-Newton DU-790N CCD. Temperature-dependent stability EL measurements of the fabricated hybrid FWLED was determined with Thorlab TED 200C temperature controller.

Results and Discussions

A schematic diagram of the FWLED is shown in Fig. 1a, along with the photograph of the substrate containing 20 active FWLEDs bent at a large angle of about 60°, while the FWLEDs remained robustly unaffected. The top view of the grown ZnO nanorods on the PFO/TFB/PEDOT:PSS flexible substrate is depicted in Fig. 2a. As can be clearly seen, a well-aligned ZnO NRs were successfully grown along their c-axial preferential growth direction. The growth of the ZnO NRs at 50°C was proved to be favorable for obtaining excellent quality ZnO NRs since this temperature is influencing both the axial length and the overall optical properties of the ZnO NRs as is discussed elsewhere [13, 14]. Figure 2b depicts the grown ZnO NRs after the photoresist was etched way. The nanorod tip in the inset of Fig. 2b is covered by photoresist with a thickness of around 40 nm, while the space between the nanorods is solidly filled by photoresist. To completely remove the photoresist coverage on the nanorods tips, the substrate was further subjected to the RIE process.

The room temperature PL spectra for the ZnO NRs grown at 50°C on bare PEDOT:PSS and on PEDOT:PSS/TFB/PFO containing multi-layers polymer hybrid inorganic/organic structure are shown in Fig. 3. The UV near band edge (NBE) emission of the ZnO NRs is clearly seen at a wavelength of about 389 nm. It is worth mentioning that the DLE frequently observed in ZnO nanostructures as well as bulk material is very weak in our 50°C grown ZnO NRs. The origin of the DLE band(s) is a controversial issue, since different defects-related transitions were assigned to be the cause of these bands e.g. the green band appeared centered around 520 nm has been attributed to various defect sources that is either point defects such as

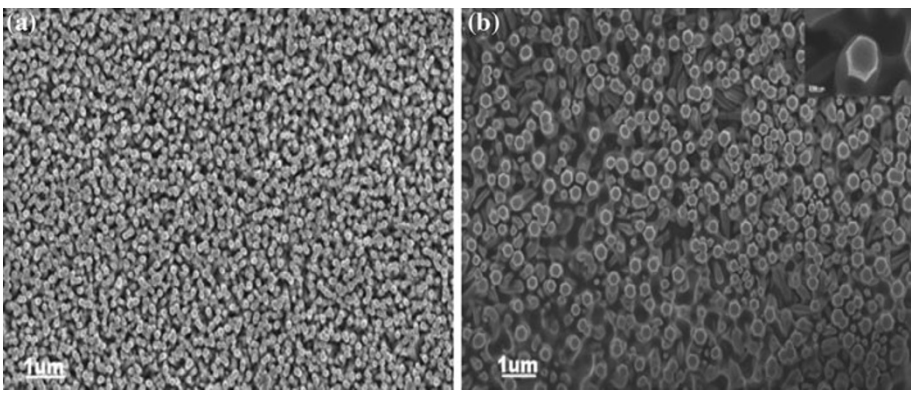

Fig. 2 Field emission scanning electron micrographs (*SEM*) of **a** ZnO nanorods grown at 50°C on TFB/PFO polymer layers on top of PEDOT:PSS/plastic flexible substrate, and in **b** SEM of the samples after photoresist processing and etching, the *inset* shows single ZnO nanorod covered by a thin photoresist film after a reactive ion etch step

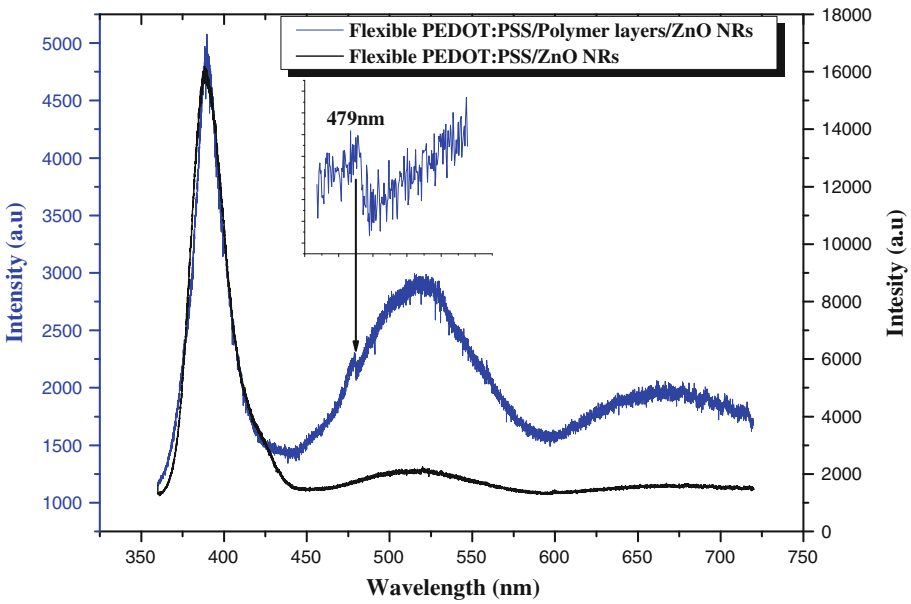

Fig. 3 Room temperature photoluminescence (*PL*) spectra from ZnO nanorods grown at 50°C on PEDOT:PSS flexible substrate (*Black*) and on TFB/PFO layers coated PEDOT:PSS (*Blue*) substrate, the *inset* shows a featured *blue peak* attribution to the PFO polymer layer

oxygen vacancies V_O, zinc vacancies V_{Zn}, or due to recombination of electrons with surface defects [15]. For more details regarding the DLE and its origin in ZnO, the reader is directed to other reviews e.g. [1, 15–17]. The red/orange band appeared around 640 nm has been also a subject of debate by many groups [15]. The PL of the PFO/TFB polymer layer on PEDOT:PSS substrate (not shown here) demonstrating multi-peak emission, centered at 430, 456, and 478 nm. These emissions have been ascribed to the light-emitting polymers TFB/PFO. The PL spectrum of the fabricated heterojunction structure of this flexible FWLED is shown in Fig. 3. It is evident that the DLE emission has been strongly enhanced in the fabricated FWLED compared to ZnO NRs grown on bare PEDOT substrate. The featured emission appeared at ~479 nm as indicated by the arrowhead in Fig. 3 is reported to be due to the 0–2 interchain singlet transition in the PFO [18].

Figure 4 shows the current–voltage (*I–V*) characteristics of the fabricated FWLED consisting of Ag/PEDOT:PSS/TFB/PFO/ZnO/Ti/Au. The *I–V* characteristics show clear diode behavior with a rectifying ratio of 6 at 5 V, and the reverse leakage current was found to be 5 μA at −15 V. The semi-log plot in Fig. 4b shows that in the low voltage regime (≤0.5 V) the *I–V* characteristic is Ohmic, above that voltage and up to ~1V the carriers tunnel through the junction and an exponential behavior becomes dominant. At higher applied voltages (≥1 V), the *I–V* retains the linear behavior again due to space charge limited current (SCLC) [4]. The general conclusion from these *I–V* curves is that this hybrid junction possesses the normal diode behavior. The energy band diagram of the device is shown

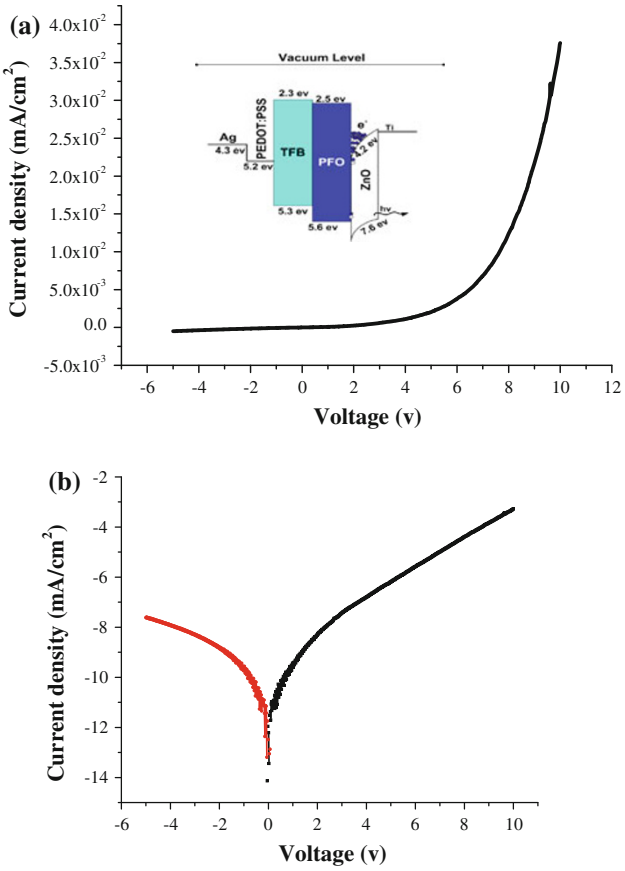

Fig. 4 Current–voltage (*I–V*) characteristics of the fabricated FWLED, in **a** a linear plot of the *I–V* demonstrating a good rectification behavior of the device. The *inset* shows the band structure diagram with offset values reported in the literature [5–7] and in **b** a semi-log plot of the *I–V* characteristics of the device

in the inset of Fig. 4a. Conductive PEDOT-PSS (ionization potential of 5.2 eV) is used as an anode and silver is used as hole injection contact. The purpose of using the TFB layer is to act as a hole transporting layer [19] and to reduce the energy barrier between the PEDOT:PSS and the PFO molecular levels, together with blocking electrons hopping from the ZnO into the PEDOT:PPS lower unoccupied molecular orbit (LUMO). This will lead to improve the device life time since hopping of carriers between large offsets will rapidly deteriorate the device performance due to generated heat. The holes under positive applied voltage tunnel across the barrier into the highest occupied molecular orbital (HOMO) levels of the PEDOT:PSS and then transported through the TFB layer that is enabling the holes to reach the PFO layer without detrimental loss as mentioned above. The potential barrier from the Ag to the HOMO level of the PEDOT:PSS and from the HOMO level of the PFO to the valence band of the ZnO NRs are 0.9 and 2.1 eV, respectively. The electron injection barriers between the Fermi level of the Ti/Au electrode and the conduction band of the ZnO nanorods and from the conduction band of the ZnO NRs and the LUMO of the PFO are 0.1 and 1.8 eV, respectively [5–7]. Due to energy band bending process the formation of sub bands take place and consequently, electrons and holes under forward bias voltages accumulate, at the PFO/ZnO interface. The electrons existing at the interface between the LUMO level of the PFO and the conduction band edge of the ZnO NRs continuously drop to the lower states and during the electron transitions continuous recombination between the electrons and holes happens leading to the emission of visible light. In addition, many radiative recombinations in the bulk of the NRs and in the bulk of the PFO also exist. The FWLED device was stored for several months and twisted in large curvatures many times as seen in Fig. 1b and then the *I–V* measurements were examined to observe the device degradation behavior. Interestingly, no increase in the turn on voltage or decrease in the output current with time and bending process were observed. The same applies to electroluminescence characteristics which will be presented below.

The room temperature electroluminescence of the FWLED is depicted on Fig. 5a, b. The device was biased at different driving voltages, and the corresponding EL spectra were recorded. The EL spectrum started to emerge at a bias voltage of 12 V along with injection current of 0.15 mA, and at 24 V a current of 1.2 mA was achieved, as can be seen in Fig. 5a. The intrinsic white light is covering the whole visible region from 420 to 800 nm as a broad peak centered at ~560 nm having a full width at half maximum (FWHM) of around 158 nm. Figure 5b displays a logarithmic scale for the broad emitted white light intensity. The intrinsic white light was clearly seen by the naked eye at a voltage of 14 V and above. It is important to mention that the TFB/PFO blue peaks are completely intermixed with the DLEs of the ZnO NRs resulting in the observed single broad band emission. On the other hand, the NBE of the ZnO NRs was not detected in the EL spectra probably due to the self-absorption of the UV light by the ZnO direct bandgap [20] or as a result of the absorption of the 389 nm NBE of the ZnO by the PFO at the PFO/ZnO NRs interface. Since the PFs polymers show a sharp absorption peak λ_{max} ~ 385–390 nm of the π–π^* electronic transition [18]. The intermixing of the blue light generated by the PFO layer with the green and red/orange bands produced by the DLE emissions in ZnO have led to the observed broad band. The effect of the PFO polymer concentration together with their processing parameters is critical in determining the overall electro-optical efficiencies and light quality of the FWLED.

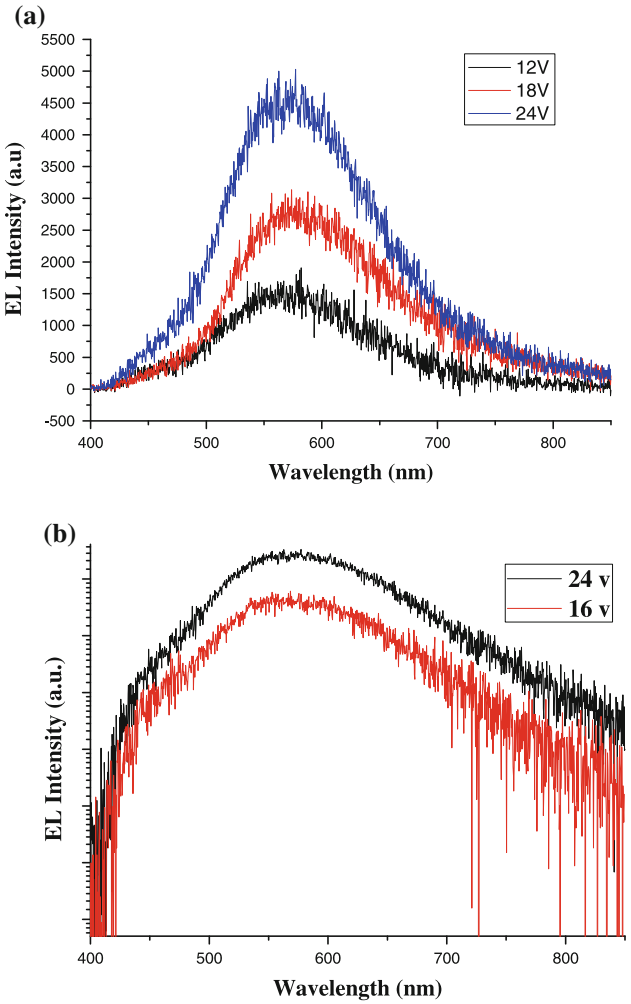

Fig. 5 Intrinsic white light electroluminescence (EL) spectra of the fabricated FWLED collected at different dc-bias as indicated, in **a** a linear-scale plot of the intensity with wavelength, and in **b** with a logarithmic scale

The device stability operation over a wide range of temperature variation is very important for real life applications in lighting and under harsh conditions. For this reason, the fabricated FWELD was examined under different temperature conditions. This was conducted inside an insulating chamber controlled via a temperature controller at temperature range 20–60°C under constant dc-bias of 20 V. The measurements were carried out 10 min after the chamber has reached the desired temperature to ensure that the FWLED also stabilized at that temperature. The results are shown in Fig. 6a (linear plot) and Fig. 6b (logarithmic plot). A gradual decrease in the EL intensity was recorded. This was attributed to the rising of the FWLED junction temperature. It is worth mentioning that no significant shift in the intrinsic white peak center position was observed as shown in Fig. 6b. Nevertheless, the FWHM started to shrink at 40 and at 60°C it was reduced to ~23% of the original value. The reduction

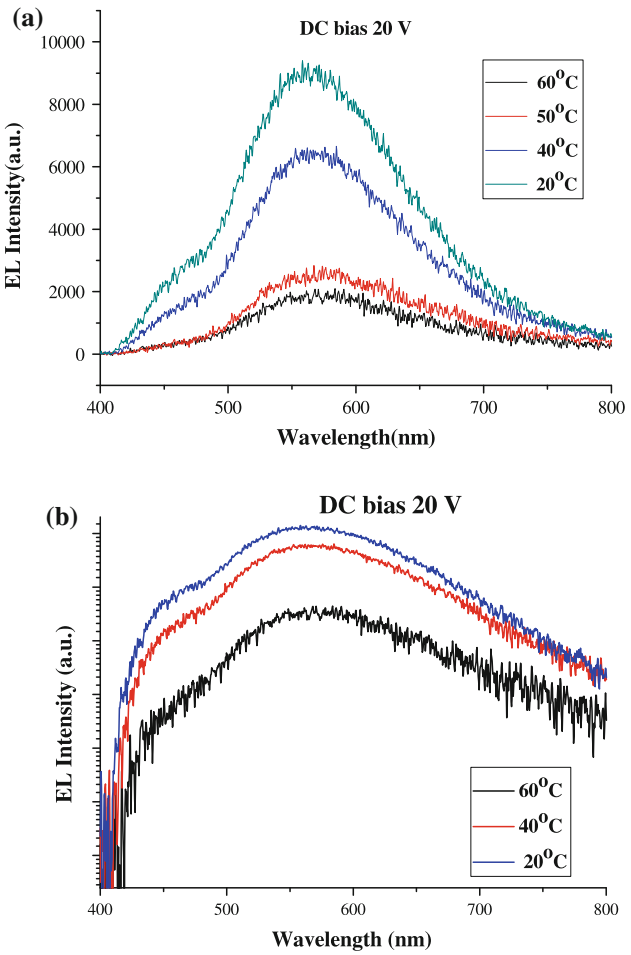

Fig. 6 Electroluminescence (EL) spectra of the FWLED at different ambient temperatures at a bias voltage of 20 V in **a** linear plot, and in **b** logarithmic scale plot, showing the depreciation of the intrinsic white light intensity with increasing the ambient temperature

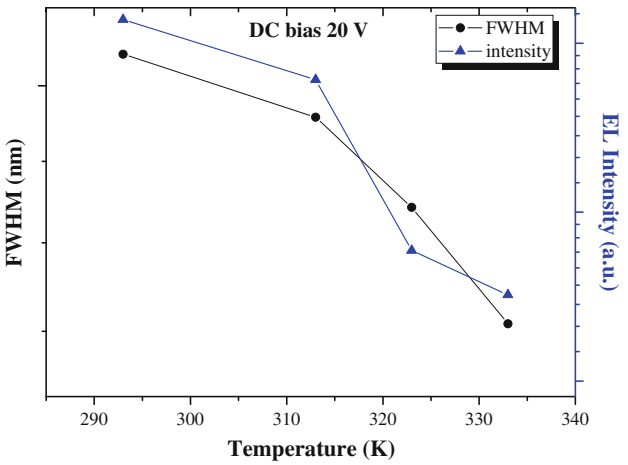

Fig. 7 The effect of the ambient temperature variations on the white light emission characteristics of the fabricated FWLED

in the EL intensity along with the effect of the temperature on the light emission FWHM is summarized in Fig. 7; the emission intensity was suppressed to ~80% by changing the device temperature from 20 to 60°C as shown in Fig. 7. The results demonstrate that our FWLED is reasonably stable over moderate temperatures, and the output light emission is unaffected by this temperature variations (20–60°C). The possible explanation of the FWLED heterojunction stability could be assigned to the low current density injection through the junction in the device. Because at higher current densities, the junction temperature will rapidly increase due to the electrons passage resulting in a faster depreciation of the device compared to ambient temperatures.

Conclusion

In summery, an intrinsic white-emitting diode was fabricated by growing well-aligned ZnO NRs at a temperature as low as 50°C following chemical bath deposition strategy. The ZnO NRs were grown on multi-layered polymers spun coated on commercially available flexible PEDOT:PSS/plastic substrate. The FWLED showed excellent *I–V* characteristics combined with single intrinsic white light extending from 420 to 800 nm. The light emission was clearly observed by the naked eye at a bias voltage of 14 V. The blue light emission from the PFO polymer layer was completely intermixed with the deep level emissions from ZnO NRs to generate single broad white light emission band. The influence of the ambient temperature on the fabricated FWLED was investigated, and the results demonstrated that the device is quite stable at elevated temperatures without showing any severe depreciation of the output light characteristics. The fabricated device was bent at large

angles (>60°) and still retained its electro-optical characteristics. This FWLED can fit well to a wide varieties of lighting applications, for instance as the substrate is highly flexible, the use of the FWLED in decoration and in-door lighting using existing armature technologies become feasible to achieve.

References

1. Ü. Özgür, Ya.I. Alivov, C. Liu, A. Teke, M.A. Reshchikov, S. Doğan, V. Avrutin, S.J. Cho, H. Morkoç, J. Appl. Phys. **98**, 041301 (2005)
2. M. Willander, O. Nur, N. Bano, K. Sultana, New J. Phys. **11**, 125020 (2009)
3. M. Willander, Q.X. Zhao, Q.-H. Hu, P. Klason, V. Kuzmin, S.M. Al-Hilli, O. Nur, E. Lozovik, Superlattices Microstructures **43**, 352 (2008)
4. A. Wadeasa, O. Nur, M. Willander, Nanotechnology **20**, 065710 (2009)
5. M. Willander, L.L. Yang, A. Wadeasa, S.U. Ali, M.H. Asif, Q.X. Zhao, O. Nur, J. Mater. Chem. **19**, 1006 (2009)
6. A. Wadeasa, S.L. Beegum, S. Raja, O. Nur, M. Willander, Appl. Phys. A **95**, 807 (2009)
7. A. Wadeasa, G. Tzamalis, P. Sehati, O. Nur, M. Fahlman, M. Willander, M. Berggren, X. Crispin, Chem. Phys. Lett. **490**, 200 (2010)
8. M. Willander, O. Nur, Q.X. Zhao, L.L. Yang, M. Lorenz, B.Q. Cao, J. Zúñiga Pérez, C. Czekalla, G. Zimmermann, M. Grundmann, A. Bakin, A. Behrends, M. Al-Suleiman, A. El-Shaer, A.C. Mofor, B. Postels, A. Waag, N. Boukos, A. Travlos, H.S. Kwack, J. Guinard, D. Si Le Dang, Nanotechnol **20**, 332001 (2009)
9. R. Könenkamp, C.W. Robert, C. Schlegel, Appl. Phys. Lett. **85**, 6004 (2009)
10. A. Nadarajah, C.W. Robert, J. Meiss, R. Könenkamp, Nano. Lett. **8**, 534 (2008)
11. C.Y. Lee, J.Y. Wang, Y. Chou, C.L. Cheng, C.H. Chao, S.C. Shiu, S.C. Hung, J.J. Chao, M.Y. Liu, Y.M. Su, Y.F. Chen, C.F. Lin, Nanotechnology **20**, 332001 (2009)
12. C. Pacholski, A. Kornowski, H. Weller, Angew. Chem. Int. Edn. **41**, 1188 (2002)
13. A. Zainelabdin, S. Zaman, G. Amin, O. Nur, M. Willander, Crystal Growth and Design (2010, submitted)
14. S. Zaman, A. Zainelabdin, O. Nur, M. Willander, J. Nanoelectron. Optoelectron. **5**, (2010)
15. A.B. Djurišic, Y.H. Leung, Small **2**, 944 (2006)
16. C. Klingshirn, Phys. Stat. Sol. **244**, 3027 (2007)
17. C. Klingshirn, Chem. Phys. Chem. **8**, 782 (2008)
18. Zhigang Li, Hong Meng, Organic light emitting materials and devices, Chap 2. (CRC Press Taylor & Francis Group 6000 Broken Sound Parkway NW, Suite 300 Boca Raton, FL 33487-2742) (2006)
19. H. Yan, Q. Huang, B.J. Scott, T.J. Marks, Appl. Phys. Lett. **84**, 3873 (2004)
20. P. Bhattacharya, Semiconductor Optoelectronic Devices, Chap 5, pp 207. (Prentice-Hall, Inc., Englewood Cliffs, NJ, USA) (1994)